

See discussions, stats, and author profiles for this publication at: <https://www.researchgate.net/publication/263944228>

Utility of Resistance and Capacitance Response in Sensors Based on Monolayer-Capped Metal Nanoparticles

ARTICLE in JOURNAL OF PHYSICAL CHEMISTRY LETTERS · JULY 2011

Impact Factor: 7.46 · DOI: 10.1021/jz2008648

CITATIONS

6

READS

6

4 AUTHORS, INCLUDING:



Yoed Tsur

Technion - Israel Institute of Technology

52 PUBLICATIONS 700 CITATIONS

[SEE PROFILE](#)



Hossam Haick

Technion - Israel Institute of Technology

158 PUBLICATIONS 4,435 CITATIONS

[SEE PROFILE](#)

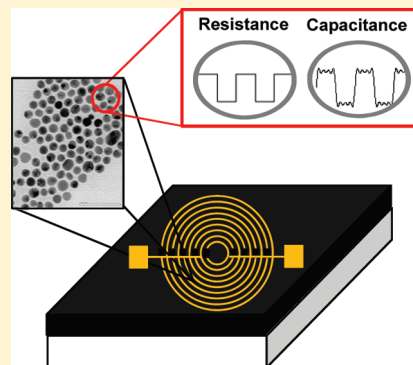
Utility of Resistance and Capacitance Response in Sensors Based on Monolayer-Capped Metal Nanoparticles

Gregory Shuster, Sioma Baltianski, Yoed Tsur, and Hossam Haick*

Department of Chemical Engineering and Russell Berrie Nanotechnology Institute, Technion – Israel Institute of Technology, Haifa 32000, Israel

 Supporting Information

ABSTRACT: We investigate the utility of resistance and capacitance responses, as derived by impedance spectroscopy, in well-controlled and real-world applications of monolayer-capped metal nanoparticle (MCNP) sensors. Exposure of the MCNP films to well-controlled analytes showed stable sensing responses and low baseline drift of the pertinent capacitance signals, when compared with equivalent resistance signals. In contrast, exposure of the MCNP films to breath of chronic kidney disease patients under dialysis, as a representative example to real-world multicomponent mixtures, showed low baseline drift but relatively scattered signals when compared with the equivalent resistance response. We ascribe these discrepancies to the level and fluctuating concentration of water molecules in the real-world samples.



SECTION: Surfaces, Interfaces, Catalysis

The use of monolayer-capped metal nanoparticles (MCNPs)^{1–2} in chemiresistors has attracted considerable attention because they are reliable, small in size and weight, simple to fabricate and operate, and fast to respond.^{1–5} Furthermore, they allow automated packaging at a wafer level as well as mass production of portable microanalysis systems with integrated read-out electronics at low costs. MCNP-based chemiresistors can be operated at room temperature or slightly above, enabling easy device integration and low power operation.⁶

So far, MCNP-based chemiresistors have been measured exclusively in DC mode or in low-frequency AC mode.^{7–9} However, for some applications, using DC mode in chemiresistors can be a disadvantage because of an inferior ability to separate between the different mechanisms involved in the sensing process. This disadvantage can be expressed by a loss of information, lower separation ability of the sensor, or false identification of different analytes.

Weimar and Göpel¹⁰ compared DC and AC setups to measure conduction properties in SO₂ as typical semiconducting gas sensors. The results of the impedance measurements showed enhancement of the sensitivity and selectivity toward various gases (H₂, CO, NO₂) when the conductance was monitored at specific frequencies. An additional example was provided by Yanez Heras et al.,¹¹ who showed that the use of impedance spectroscopy in conjugation with principal component analysis allowed trace detection of metal ions using a sensor-based chelating agent (pyrocatechol violet and a nitrilotriacetic derivative). The system was able to differentiate eight metal ions (Al³⁺, Fe³⁺, Cd²⁺, Pb²⁺, Hg²⁺, Cu²⁺, Ca²⁺, and Ag⁺) at micromolar levels in ultrapure water and without effects of confounding factors.

In this Letter, we investigate the utility of resistance and capacitance measurements in well-controlled and real-world applications of MCNP sensors. We do so by comparing the resistance and capacitance responses derived in each case and by analyzing the constituent signal's magnitude as well as the drift over time. Pattern recognition methods are used for convenient comparison between large sets of data collected in each case.

Figure 1a shows an impedance measurement for a 2-mercapto-benzylalcohol-AuNP (MBA-AuNP) sensor upon exposure to hexane as a representative example. The signal obtained was then fitted to RC circuit impedance (solid lines) using the following equations

$$Re(Z)_{\text{fit}} = \frac{R}{1 + \omega^2 \tau^2} \quad (1)$$

$$Im(Z)_{\text{fit}} = -\frac{R\omega\tau}{1 + \omega^2 \tau^2} \quad (2)$$

where $\tau = RC$ and ω is the angular frequency. As seen in Figure 1a, the impedance measurements of the MBA-AuNP sensor (dots) were well-described by the RC circuit (solid lines).¹² The measured DC resistance was consistent with the resistance derived from the impedance measurement (as expected from the RC circuit model). Representative changes in the resistance and capacitance responses upon subsequent exposure to dry air, hexane, hexanol, and dry air are presented in Figure 1b. As the Figure shows, the magnitude of the capacitance response,

Received: June 27, 2011

Accepted: July 14, 2011



ACS Publications

© XXXX American Chemical Society

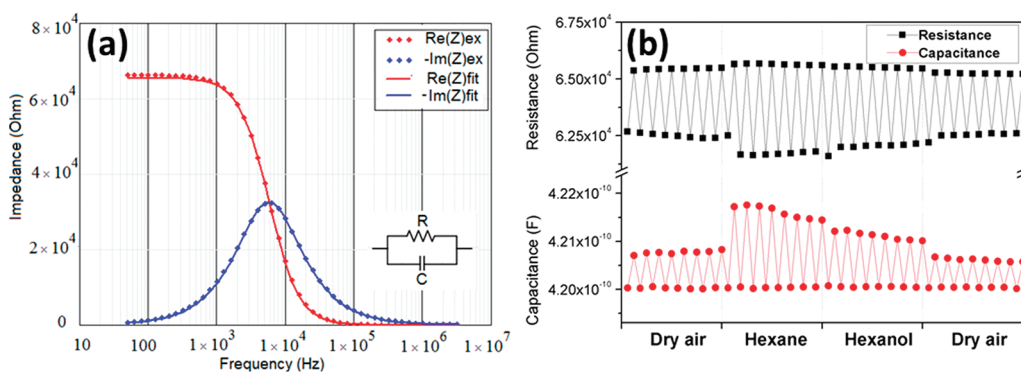


Figure 1. (a) Real and imaginary parts of the MBA-AuNP's impedance signal upon exposure to hexane. Dotted lines present the experimental results, and solid lines present the fitting to a single RC circuit. According to the fitting, the resistance and the capacitance of the MBA-AuNP film are $R = 6.55 \times 10^4 \Omega$ and $C = 4.22 \times 10^{-10} \text{ F}$, respectively. Inset: A simplified RC model circuit with a resistor and a capacitor in parallel. (b) Representative resistance and capacitance responses upon exposure of the MBA-AuNP to different analytes. For each analyte, the exposure was repeated eight times. The chamber was cleaned by vacuum pump between each gas introduction. The first step (first point in the graph) is vacuum.

Table 1. PC1 Component of the PCA Analysis for the Resistance and the Capacitance Responses

cycle no.	model derived resistance				model-derived capacitance			
	dry air, first cycle	hexane	hexanol	dry air, last cycle	dry air, first cycle	hexane	hexanol	dry air, last cycle
1	-3.27	1.98	2.97	-2.01	-2.38	5.10	1.38	-2.68
2	-2.67	4.75	1.80	-3.13	-2.09	5.40	1.31	-2.87
3	-2.20	4.69	1.53	-3.35	-2.00	5.25	0.93	-3.05
4	-1.88	4.46	1.23	-3.53	-2.08	4.73	0.67	-3.13
5	-1.53	4.14	1.07	-3.76	-1.88	3.90	0.39	-3.24
6	-1.18	3.80	0.86	-3.83	-1.81	3.38	0.14	-3.34
7	-1.19	3.52	0.55	-3.84	-1.65	3.19	-0.18	-3.39
mean	-1.99	3.90	1.43	-3.35	-1.98	4.42	0.66	-3.10
stdev	0.78	0.96	0.80	0.65	0.24	0.92	0.59	0.25

compared with the resistance response, exhibited better stability and high uniformity throughout the eight exposure repetitions. Furthermore, the drift in the capacitance baseline was much lower than that for the resistance baseline, thus allowing more reproducible results. To support this conclusion, principle component analysis (PCA) was carried out. For the purpose of the current study, PCA transforms the resistance and capacitance data to common unitless dimensions of PC1 while presenting the variance within the data. As such, one can compare the different PC1 mean values for each analyte and the standard deviation of those values. As seen in Table 1, the capacitance response provided slightly better uniformity between the varying exposures to dry air compared with the resistance response. This difference could be attributed to smaller drift in the sensor's capacitance during the exposure process. The capacitance response provided lower standard deviation for all tested analytes, implying a higher stability and responses with less drift. Finally, the difference between the PC1 values upon exposure to hexane and the PC1 values upon exposure to hexanol was much higher in capacitance response compared with the resistance response. This implies that capacitance allows better discrimination between hexane and hexanol.

The lower drift in the capacitance baseline could be attributed to the morphology of the MBA-AuNP film. As shown in Figure 2, the MBA-AuNP film consists of high density and low density

areas. Under steady-state conditions, the dense areas would accumulate residues of analytes that were not fully removed during the (prior) vacuum step. Consequently, the analyte residues affect the carrier tunneling between the adjacent MBA-AuNPs, affecting the constituent MBA-Au NP film baseline resistance.¹² The low density areas are characterized by larger spacing between the adjacent MBA-AuNPs, where the carrier tunneling is negligible¹³ and the overall contribution to the impedance is mainly due to the capacitive charging of the MBA-AuNPs. In these areas, the analyte residues, which are easily removed during the vacuum step, would have negligible effect on the constituent capacitance.

The capacitance and resistance responses were examined for monitoring chronic kidney disease (CKD) states during dialysis sessions using exhaled breath samples, as a representative example for real-world multicomponent mixtures. Generally speaking, exhaled breath samples contain nitrogen, oxygen, carbon dioxide, and thousands of trace-level volatile organic compounds that appear in parts per billion to parts per trillion levels. The breath VOCs are generated by the cellular biochemical processes of the body or are absorbed from the environment through ingestion, through inhalation, or through skin contact. These processes may cause specific volatile organic compounds to be emitted into the blood and, subsequently, into the alveolar exhaled breath through exchange via the lung. However, the high

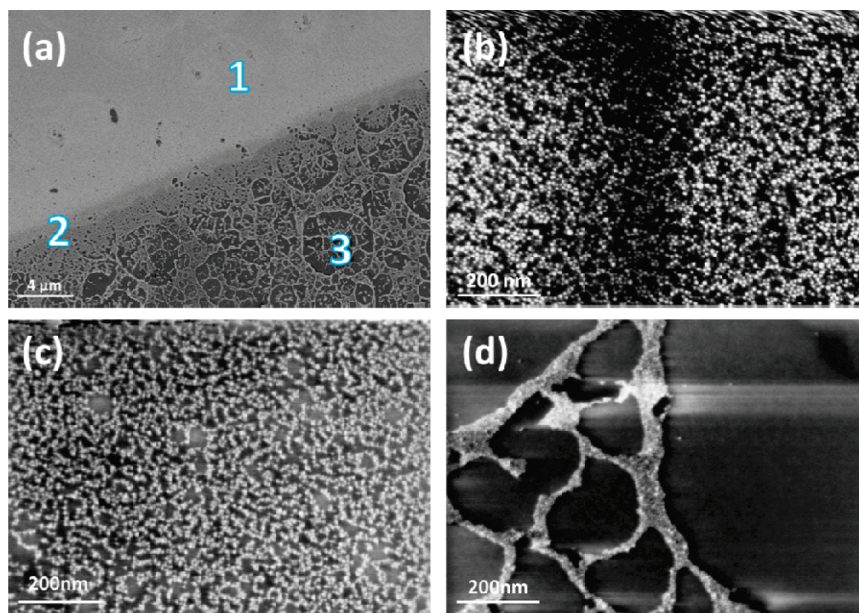


Figure 2. (a) Scanning electron microscopy (SEM) images of the MBA-AuNP film. The morphology of the MBA-AuNPs changes from high density areas (1) through medium-dense areas (2) to the low density areas having net-like structure (3). (b) Magnification of area 1. (c) Magnification of area 2. (d) Magnification of area 3.

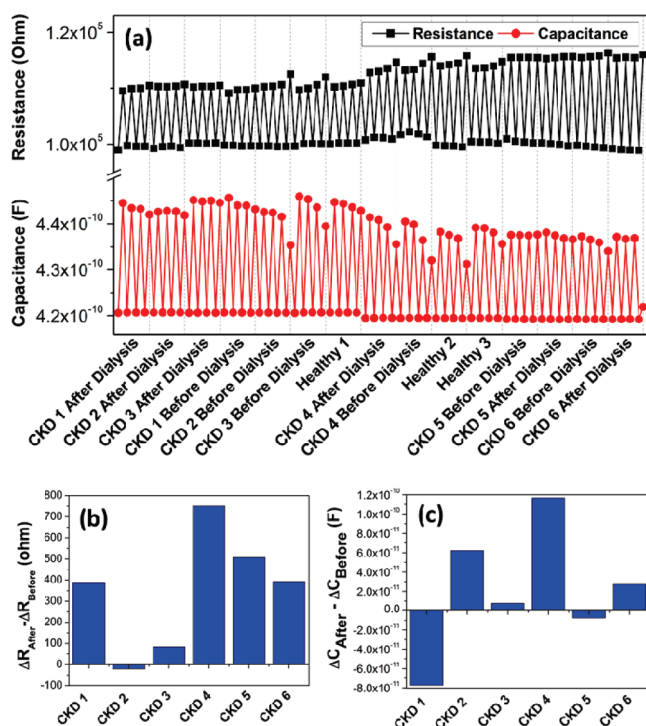


Figure 3. (a) Representative resistance and capacitance responses of the MBA-AuNP sensor upon exposure to 15 breath samples, obtained over a period of ~1 month on three different days of sample measurement. The first step (first point in the graph) is vacuum. Each breath sample was measured four times. Between each breath sample introduction, the chamber was cleaned using a vacuum pump, which also serves as baseline of the sensor's resistance/capacitance between exposures. (b) Difference between the responses to breath samples collected before and after dialysis according to the resistance measurements. (c) Difference between the responses to breath samples collected before and after dialysis according to the capacitance measurements.

relative humidity (RH) in the breath samples (>80% RH, equivalent to >25 000 ppm of water vapor at 1 atm and 25 °C)¹⁴ usually screens the disease-related polar and nonpolar volatile organic compounds,¹⁵ thus limiting the accuracy of the analysis.^{16,17}

Figure 3a presents resistance and capacitance responses, as derived from the RC circuit model (eqs 1 and 2) upon exposure to CKD and healthy breath samples. Each breath sample allowed filling the chamber four times. As the Figure shows, the resistance baseline was noisy and was accompanied by a drift. The capacitance baseline did not change during the entire experiment period, except one minor change between the first and the second day. Figures 3b and 3c present, respectively, the difference between the resistance and capacitance responses for each CKD subject before and after dialysis. As seen in these figures, the resistance response of the postdialysis was higher than the predialysis in five of six cases (83%), indicating a satisfactory capability for monitoring dialysis process. The capacitance response exhibited high variance from sample to sample and correct classification of four of six cases (67%). This observation could be explained by the higher signal-to-noise ratio in the resistance response compared with the capacitance response. Indeed, the latter is affected by the high concentration of water molecules in the breath samples. It is likely that the higher dielectric constant of water (78.5), the high concentration of water molecules, and the significant variability of water content from sample to sample, screens the capacitance effect of the volatile organic compounds present in the sample (mostly characterized by a dielectric constant <10). Nevertheless, tailoring the MBA-AuNP sensors in a manner that would give a higher signal-to-noise ratio in the capacitance part or lower sensitivity to water molecules would contribute additional information to the analysis of real breath samples.

The higher responses obtained in the postdialysis session, compared with the predialysis session (Figure 3b and 3c), could

be attributed to the semiselectivity of the MBA-AuNP film to adsorb and detect breath volatile organic compounds that are produced during the dialysis session. Preliminary gas chromatography linked to mass spectrometry analysis for CKD breath samples showed that the concentration of a few materials, such as isoprene, acetone, acetic acid, and some amine derivatives, is higher after the dialysis process than before the dialysis process, most probably because of fasting. A detailed paper on these findings will be published elsewhere.

In summary, capacitance response of MBA-AuNP films exhibited higher signal-to-noise ratio and lower baseline drift than the equivalent resistance response upon exposure to well-controlled and water-free samples. In contrast, the capacitance response of the MBA-AuNP film exhibited low signal-to-noise ratio and low baseline drift upon exposure to real-world multi-component mixtures, namely, breath of CKD patients. These discrepancies were attributed to the higher screening effect of the water molecules on the capacitance part of the sensor. These findings imply that impedance spectroscopy allows us to tailor the electrical features of the MCNP sensors based on the application of interest. Nevertheless, impedance spectroscopy experiments with a wider range of cross-reactive MCNP films, MCNP morphologies, analytes, and concentrations should be examined to validate statistically these conclusions.

■ EXPERIMENTAL METHODS

Chemiresistors based on 3–5 nm gold nanoparticles (Au NP) coated with 2-mercapto-benzylalcoholthiol ligand (MBA-AuNP; see the Supporting Information for a representative transmission electron micrograph) films were fabricated as previously described.^{18,19} The chemiresistors were dried in vacuum for an overnight period. The MBA-AuNP sensor was placed in a glass chamber. The glass chamber was then fitted with entrance/exit gas lines, a rotation vacuum pump (GE Motors & Industrial Systems, MOD SK36GN166), a pressure meter (NFZ k.I 1.6), and electrical connections to a precision impedance analyzer (Agilent 4294A), used at frequency range from 50 Hz to 3 MHz, and to a source meter (Keithley 2400) for DC resistance measurements. The level of signal excitation of both device analyzers was 0.5 V rms. Switching between the two devices was done using a switch/control system (Agilent 3499A).²⁰ Using this setup, the MBA-AuNP sensors were exposed to dry air (<100 ppb organic contamination), to 50 ppm hexane as a representative nonpolar compound, and to 11 ppm hexanol as a representative polar compound. All compounds were produced using a Zero-Air device (MCZ 2000-25 MD; Umwelttechnik MCZ GmbH, Germany) that was connected to a compatible dilution module (IC 2000 RL, Umwelttechnik MCZ GmbH, Germany) and to a compatible humidifier module. Together, these systems could produce controlled gas flow of desired gas mixtures in clean air at a determined concentration and RH % level.

To study the efficiency of the impedance measurements in real-world sensing applications, a small scale clinical trial was conducted. Twelve breath samples were collected from six volunteers suffering from stage-5 CKD and exposed to the MBA-Au NP sensors. All volunteers with the disease were recruited from the Department of Nephrology of the Rambam Healthcare Campus (Haifa, Israel), during their routine visits for dialysis sessions. Breath samples were collected from each volunteer 15 min after the beginning of the dialysis session and

15 min before the end of the dialysis session. Ethical approval was obtained from the Rambam Healthcare Campus and Technion's committee for supervision of human experiments (Haifa, Israel). The breath collection was carried out as described earlier.²¹ For each exposure experiment, the DC resistance and impedance were measured nine times in each of the vacuum and exposure steps. The capacitance and AC resistance were derived from impedance measurements using the Impedance Spectroscopy Genetic Programming (ISGP) program.^{22,23} This program seeks the underlying time constant distribution function using an evolutionary programming method. A simple RC circuit would result in a delta function as its distribution. The ISGP finds a slightly better fit for a narrow Pearson VII type peak. Since this peak width is even smaller than the reciprocal of the frequency step size, it is justified to use the single RC approximation.

■ ASSOCIATED CONTENT

Supporting Information. Transmission electron microscope image of the MBA-AuNPs. This material is available free of charge via the Internet at <http://pubs.acs.org>.

■ AUTHOR INFORMATION

Corresponding Author

*E-mail: hhossam@technion.ac.il

■ ACKNOWLEDGMENT

We acknowledge the financial support from the Marie Curie Excellence Grant of the FP6 and FP7-HEALTH Programs of the European Commission. S.B. wishes to thank the Center for Absorption in Science (Ministry of Immigrant Absorption) for its support. We wish to acknowledge Mr. Ophir Marom for the help in collection of breath samples and the GC-MS analysis. H. H. is a Knight of the Order of Academic Palms and holds the Horev Chair for Leaders in Science and Technology.

■ REFERENCES

- Daniel, M. C.; Astruc, D. Gold Nanoparticles: Assembly, Supramolecular Chemistry, Quantum-Size-Related Properties, and Applications toward Biology, Catalysis, and Nanotechnology. *Chem. Rev.* **2004**, *104*, 293–346.
- Haick, H. Chemical Sensors Based Molecularly Modified Metallic Nanoparticles. *J. Phys. D* **2007**, *40*, 7173–7186.
- Tisch, U.; Haick, H. Nanomaterials for Cross-Reactive Sensor Arrays. *MRS Bull.* **2010**, *35*, 797.
- Joseph, Y.; et al. Self-Assembled Gold Nanoparticle/Alkanethiol Films: Preparation, Electron Microscopy, XPS-Analysis, Charge Transport, and Vapor-Sensing Properties. *J. Phys. Chem. B* **2003**, *7406–7413*.
- Toda, M.; Joseph, Y.; Berger, R. Swelling of Composite Films at Interfaces. *J. Phys. Chem.* **2010**, *114*, 2012–2017.
- Schöning, M. J. “Playing Around” with Field-Effect Sensors on the Basis of Eis Structures, Laps and Isfets. *Sensors* **2005**, *5*, 126–138.
- Guo, J.; Pang, P.; Cai, Q. Effect of Trace Residual Ionic Impurities on the Response of Chemiresistor Sensors with Dithiol-Linked Monolayer-Protected Gold (Nano)Clusters as Sensing Interfaces. *Sens. Actuators, B* **2007**, *120*, 521–528.
- Joseph, Y.; Guse, B.; Vossmeyer, T.; Yasuda, A. Gold Nanoparticle/Organic Networks as Chemiresistor Coatings: The Effect of Film Morphology on Vapor Sensitivity. *J. Phys. Chem. C* **2008**, *112*, 12507–12514.
- Wuelfing, W. P.; Murray, R. W. Electron Hopping through Films of Arenethiolate Monolayer-Protected Gold Clusters. *J. Phys. Chem. B* **2002**, *106*, 3139–3145.

- (10) Weimar, U.; Gopel, W. AC Measurements on Tin Oxide Sensors to Improve Selectivities and Sensitivities. *Sens. Actuators, B* **1995**, *26*, 13–18.
- (11) Yanez Heras, J.; Rodriguez, S. D.; Negri, R. M.; Battaglini, F. Chelating Electrodes as Taste Sensor for the Trace Assessment of Metal Ions. *Sens. Actuators, B* **2010**, *145*, 726–733.
- (12) Zabet-Khosousi, A.; Dhirani, A. Charge Transport in Nanoparticle Assemblies. *Chem. Rev.* **2008**, *108*, 4072–4124.
- (13) Torma, V.; Schmid, G.; Simon, U. Structure-Property Relations in Au55 Cluster Layers Studied by Temperature-Dependent Impedance Measurements. *ChemPhysChem* **2001**, *2*, 321–325.
- (14) Beauchamp, J.; Herbig, J.; Gutmann, R.; Hansel, A. On the Use of Tedlar Bags for Breath-Gas Sampling and Analysis. *J. Breath Res.* **2008**, *2*, 046001.
- (15) Zilberman, Y.; Tisch, U.; Shuster, G.; Pisula, W.; Feng, X.; Müllen, K.; Haick, H. Carbon Nanotube/Hexa-Peri-Hexabenzocoronene Bilayers for Discrimination between Nonpolar Volatile Organic Compounds of Cancer and Humid Atmospheres. *Adv. Mater.* **2010**, *22*, 4317–4320.
- (16) Patel, S. V.; Jenkins, M. W.; Hughes, R. C.; Yelton, W. G.; Ricco, A. J. Differentiation of Chemical Components in a Binary Solvent Vapor Mixture Using Carbon/Polymer Composite-Based Chemiresistors. *Anal. Chem.* **2000**, *72*, 1532–1542.
- (17) Peng, G.; Trock, E.; Haick, H. Detecting Simulated Patterns of Lung Cancer Biomarkers by Random Network of Single-Walled Carbon Nanotubes Coated with Nonpolymeric Organic Materials. *Nano Lett.* **2008**, *8*, 3631–3635.
- (18) Peng, G.; Tisch, U.; Adams, O.; Hakim, M.; N., S.; Billan, S.; Abdah-Bortnyak, R.; Kuten, A.; Haick, H. Diagnosing Lung Cancer in Exhaled Breath Using Gold Nanoparticles. *Nature Nanotechnol.* **2009**, *4*, 669–673.
- (19) Peng, G.; Hakim, M.; Broza, Y. Y.; Billan, S.; Abdah-Bortnyak, R.; Kuten, A.; Tisch, U.; Haick, H. Detection of Lung, Breast, Colorectal, and Prostate Cancers from Exhaled Breath Using a Single Array of Nanosensors. *Br. J. Cancer* **2010**, *103*, 542–551.
- (20) Melman, Y.; Baltianski, S.; Tsur, Y. A Device for Measuring Electrical Properties of Dielectric Materials. *Instrum. Sci. Technol.* **2005**, *33*, 279–287.
- (21) Shuster, G.; et al. Classification of Breast Cancer Precursors through Exhaled Breath. *Breast Cancer Res. Treat.* **2011**, *126*, 791–796.
- (22) Tesler, A. B.; Lewin, D. R.; Baltianski, S.; Tsur, Y. Analyzing Results of Impedance Spectroscopy Using Novel Evolutionary Programming Techniques. *J. Electroceram.* **2010**, *24*, 245–260.
- (23) Hershkovitz, S.; Baltianski, S.; Tsur, Y. Harnessing Evolutionary Programming for Impedance Spectroscopy Analysis: A Case Study of Mixed Ionic-Electronic Conductors. *Solid State Ionics* **2011**, *188*, 104–109.